

Normal-moveout velocity and generalized Dix equation for inhomogeneous anisotropic media

*Vladimir Grechka, Ilya Tsvankin, and Jack K. Cohen
Center for Wave Phenomena, Department of Geophysics,
Colorado School of Mines, Golden, CO 80401-1887*

ABSTRACT

Despite the complexity of wave propagation in anisotropic media, reflection moveout on conventional common-midpoint (CMP) spreads is usually well described by the normal-moveout (NMO) velocity defined in the zero-spread limit. In their recent work, Grechka and Tsvankin showed that the azimuthal dependence of NMO velocity generally has an *elliptical* shape and is determined by the spatial derivatives of the slowness vector evaluated at the CMP location. This formalism is used here to develop exact solutions for normal-moveout velocity in anisotropic media of arbitrary symmetry.

For the model of a single homogeneous layer above a dipping reflector, we obtain an *explicit* NMO expression valid for all pure modes and any orientation of the CMP line with respect to the reflector strike. The influence of anisotropy on normal-moveout velocity is absorbed by the slowness components of the zero-offset ray (along with the derivatives of the vertical slowness with respect to the horizontal slownesses) – quantities that can be found in a straightforward way from the Christoffel equation. If the overburden is horizontally layered, the effective NMO velocity is determined through a Dix-type average of the matrices responsible for the “interval” NMO *ellipses* in the individual layers. This generalized Dix equation provides an analytic basis for moveout inversion in vertically inhomogeneous, arbitrary anisotropic media. For models with a throughgoing vertical symmetry plane (i.e., if the dip plane of the reflector coincides with a symmetry plane of the overburden), the semi-axes of the NMO ellipse are found by the more conventional rms averaging of the interval NMO *velocities* in the dip and strike directions.

Modeling of normal moveout in the most general heterogeneous anisotropic media requires *dynamic* ray tracing of only *one* (zero-offset) ray. Remarkably, the expressions for geometrical spreading along the zero-offset ray contain all the components necessary to build the NMO ellipse. This method is orders of magnitude faster than multi-azimuth, multi-offset ray tracing and, therefore, can be efficiently used in traveltime inversion and in devising fast dip-moveout (DMO) processing algorithms for anisotropic media. Furthermore, if the model consists of homogeneous layers or blocks separated by smooth interfaces, the quantities needed for NMO-velocity computation can be obtained from *kinematic* ray tracing alone. The high accuracy of our semi-analytic algorithm is illustrated by a comparison with ray-traced reflection traveltimes in piecewise-homogeneous, azimuthally anisotropic models.

INTRODUCTION

Reflection moveout in inhomogeneous anisotropic media is usually calculated by multi-offset and multi-azimuth ray tracing (e.g., Gajewski and Pšenčik, 1987). While

the existing anisotropic ray-tracing codes are sufficiently fast for forward modeling, their application in moveout inversion requires repeated generation of azimuthally-dependent traveltimes around many common-midpoint (CMP) locations, which makes the inversion procedure extremely time-consuming.

Moveout modeling, however, can be simplified by taking advantage of the limited range of offsets in conventional acquisition design. For common spreadlength-to-depth ratios close to unity, CMP traveltimes in media with moderate structural complexity are well described by the normal-moveout (NMO) velocity defined in the zero-spread limit (Tsvankin and Thomsen, 1994; Grechka and Tsvankin, 1996). Even if the data exhibit nonhyperbolic moveout, NMO velocity is still responsible for the most stable, small-offset portion of the moveout curve, which can be used to obtain an initial velocity model for inversion.

Existing methods for computing normal-moveout velocity are designed for inhomogeneous isotropic media (e.g., Shah, 1973; Hubral and Krey, 1980). Angular velocity variations in anisotropic models make both analytic and computational aspects of NMO-velocity modeling much more complicated. Here, we present an analytic treatment of NMO velocity in inhomogeneous anisotropic media that leads to a dramatic increase in the efficiency of traveltimes modeling methods and helps to develop insight into the influence of the anisotropic parameters on reflection traveltimes.

Explicit expressions for normal-moveout velocity are well known for the relatively simple transversely isotropic model with a vertical symmetry axis (VTI media) (e.g., Hake et al., 1984; Thomsen, 1986). Recently, Tsvankin (1995) presented an exact NMO equation for dipping reflectors valid in vertical symmetry planes of any homogeneous anisotropic medium. Alkhalifah and Tsvankin (1995) extended this result by developing a Dix-type equation for vertically *inhomogeneous* anisotropic media above a dipping reflector. They also showed that the NMO-velocity function in VTI media depends on just two parameters – the zero-dip NMO velocity $V_{\text{nmo}}(0)$ and the “anellipticity” coefficient η . Still, their formalism is limited to 2-D wave propagation in the dip plane of the reflector, which should also coincide with a symmetry plane of the overburden.

This work is based on a general 3-D treatment of normal moveout developed by Grechka and Tsvankin (1996), who proved that the azimuthal dependence of NMO velocity for pure (non-converted) modes has an *elliptical* shape in the horizontal plane, even if the medium is arbitrary anisotropic and inhomogeneous. This conclusion breaks down only for subsurface models in which common-midpoint reflection traveltimes cannot be described by a series expansion or does not increase with offset. The orientation of the NMO ellipse and the values of its semi-axes can be expressed through the spatial derivatives of the slowness vector, which are determined by both the direction of the reflector normal and the medium properties above the reflector. Grechka and Tsvankin (1996) also obtained explicit representations of the NMO velocity for dipping reflectors beneath VTI media and a horizontal orthorhombic layer. A detailed analysis of the NMO ellipse for transversely isotropic media with a hori-

zonal symmetry axis (HTI media) is given in Tsvankin (1997), who also discusses the inversion of conventional-spread reflection moveout for the parameters of HTI media.

Here, we apply the normal-moveout equation of Grechka and Tsvankin to more complicated anisotropic models. We start by deriving an explicit expression for azimuthally-dependent NMO velocity from a dipping reflector overlaid by a homogeneous layer of arbitrary symmetry. Then we obtain a generalized Dix equation for NMO velocity in a model composed of a stack of horizontal homogeneous, arbitrarily-anisotropic layers above a dipping reflector. While this equation has a form similar to the conventional Dix formula, it is based on the averaging of the *matrices* that define interval NMO *ellipses*. Finally, we present an efficient methodology to compute the normal-moveout velocity in the most general inhomogeneous media using the dynamic ray-tracing of only *one* (zero-offset) ray. We show that the derivatives needed to find the geometrical spreading (e.g., Červený, Molotkov and Pšenčík, 1977; Kendall and Thomson, 1989) provide sufficient information to build the NMO ellipse and, therefore, model reflection moveout without tracing a large family of rays.

EQUATION OF THE NMO ELLIPSE

Suppose the traveltimes of a certain reflected wave (“reflection moveout”) have been recorded on a number of common-midpoint (CMP) gathers with different azimuthal orientation but the same midpoint location. If the medium is anisotropic and inhomogeneous, the dependence of large-offset reflection traveltimes on the azimuth α of the CMP line may become rather complicated. For conventional spreadlengths close to the distance between the CMP and the reflector, however, moveout in CMP geometry is usually well-approximated by a hyperbolic equation,

$$t^2(\alpha) \approx t_0^2 + \frac{x^2}{V_{\text{nmo}}^2(\alpha)}. \quad (1)$$

Here t_0 is the zero-offset reflection time, x is the source-receiver offset, and $V_{\text{nmo}}(\alpha)$ is the normal-moveout velocity defined as

$$V_{\text{nmo}}^2(\alpha) = \lim_{x \rightarrow 0} \frac{d(x^2)}{d(t^2)}. \quad (2)$$

Thus, conventional-spread reflection moveout around a given CMP location is determined by the azimuthally-varying normal-moveout velocity. The analysis below is based on the general result of Grechka and Tsvankin (1996), who showed that NMO velocity is described by the following simple quadratic form:

$$V_{\text{nmo}}^{-2}(\alpha) = W_{11} \cos^2 \alpha + 2 W_{12} \sin \alpha \cos \alpha + W_{22} \sin^2 \alpha, \quad (3)$$

where \mathbf{W} is a symmetric matrix defined as

$$W_{ij} = \tau_0 \left. \frac{\partial^2 \tau}{\partial x_i \partial x_j} \right|_{\mathbf{x}_{\text{CMP}}} = \tau_0 \left. \frac{\partial p_i}{\partial x_j} \right|_{\mathbf{x}_{\text{CMP}}}, \quad (i, j = 1, 2). \quad (4)$$

Here, $\tau(x_1, x_2)$ is the *one-way* traveltimes from the zero-offset reflection point to some location $\mathbf{x} \{x_1, x_2\}$ at the surface, τ_0 is the one-way zero-offset traveltimes, p_i are the components of the slowness vector corresponding to the ray emerging at the point \mathbf{x} , and \mathbf{x}_{CMP} is the CMP location; the origin of the coordinate system in the derivations below coincides with the zero-offset reflection point. The one-way traveltimes appear in equation (4) because reflection-point dispersal has no influence on the NMO velocity of pure modes, and (for the small source-receiver offsets appropriate for estimation of V_{nmo}) rays can be assumed to propagate through the reflection point of the zero-offset ray (Hubral and Krey, 1980; Tsvankin, 1995).

It is convenient to use the eigenvectors of the matrix \mathbf{W} as auxiliary horizontal axes and rotate the NMO equation (3) by the angle β (see Appendix A),

$$\beta = \tan^{-1} \left[\frac{W_{22} - W_{11} + \sqrt{(W_{22} - W_{11})^2 + 4W_{12}^2}}{2W_{12}} \right]. \quad (5)$$

This rotation reduces equation (3) to

$$V_{\text{nmo}}^{-2}(\alpha) = \lambda_1 \cos^2(\alpha - \beta) + \lambda_2 \sin^2(\alpha - \beta), \quad (6)$$

where $\lambda_{1,2}$ are the eigenvalues of the matrix \mathbf{W} . Grechka and Tsvankin (1996) conclude that for positive λ_1 and λ_2 the NMO velocity (3) represents an *ellipse* in the horizontal plane. A negative eigenvalue implies a negative V_{nmo}^2 in certain azimuthal directions and, consequently, a decrease in the CMP traveltimes with offset. Although such reverse moveout can exist in some cases (e.g., for turning waves, as described by Hale et al., 1992), typically both λ_1 and λ_2 are positive, and the azimuthal dependence of NMO velocity is indeed elliptical. Note that this conclusion is valid for arbitrary inhomogeneous anisotropic media provided the traveltimes field is sufficiently smooth to be adequately approximated by a Taylor series expansion.

HOMOGENEOUS ARBITRARY ANISOTROPIC LAYER

General case

To obtain normal-moveout velocity for any given model from equations (3) and (4), we need to evaluate the spatial derivatives of the slowness vector at the CMP location. As demonstrated in Appendix B, for the model of a single homogeneous layer this can be done by representing the horizontal ray displacement through group velocity and using the relation between the group-velocity and slowness vectors. As a result, we find the following explicit expressions for the matrix \mathbf{W} and azimuthally-dependent NMO velocity [equations (B-8) and (B-10)]:

$$\mathbf{W} = \frac{p_1 q_{,1} + p_2 q_{,2} - q}{q_{,11} q_{,22} - q_{,12}^2} \begin{pmatrix} q_{,22} & -q_{,12} \\ -q_{,12} & q_{,11} \end{pmatrix}, \quad (7)$$

$$\begin{aligned}
V_{\text{nmo}}^2(\alpha) &\equiv V_{\text{nmo}}^2(\alpha, p_1, p_2) \\
&= \frac{q_{,11}q_{,22} - q_{,12}^2}{p_1q_{,1} + p_2q_{,2} - q} \left[q_{,22} \cos^2 \alpha - 2q_{,12} \sin \alpha \cos \alpha + q_{,11} \sin^2 \alpha \right]^{-1}, \quad (8)
\end{aligned}$$

where $q \equiv q(p_1, p_2) \equiv p_3$ denotes the vertical slowness component, $q_{,i} \equiv \partial q / \partial p_i$, and $q_{,ij} \equiv \partial^2 q / \partial p_i \partial p_j$; the horizontal components of the slowness vector (p_1 and p_2) in equation (8) are evaluated for the zero-offset ray.

Equation (8) is valid for pure modes reflected from horizontal or dipping interfaces in media with arbitrary symmetry and any strength of the anisotropy. The normal-moveout velocity is fully determined by the azimuth α of the CMP line and the horizontal slowness components of the zero-offset ray which, in turn, depend on the dip and azimuth of the reflector. (The slowness vector of the zero-offset ray is normal to the reflecting interface.) The vertical slowness component $q = q(p_1, p_2)$ should be found from the Christoffel equation, which can be reduced to the form $F(q, p_1, p_2) = 0$, where F is (in general) a sixth-order polynomial with respect to q (see the section on ray theory below). Then the derivatives $q_{,i}$ and $q_{,ij}$ can be obtained by implicit differentiation as

$$q_{,i} = -\frac{F_{p_i}}{F_q}$$

and

$$q_{,ij} = -\frac{F_{p_i p_j} + F_{p_i q} q_{,j} + F_{p_j q} q_{,i} + F_{qq} q_{,i} q_{,j}}{F_q}, \quad (9)$$

where $F_{p_i} \equiv \partial F / \partial p_i$, $F_q \equiv \partial F / \partial q$, $F_{p_i p_j} \equiv \partial^2 F / \partial p_i \partial p_j$, $F_{p_i q} \equiv \partial^2 F / \partial p_i \partial q$, and $F_{qq} \equiv \partial^2 F / \partial q^2$.

If the medium has a horizontal symmetry plane (e.g., it may be transversely isotropic, orthorhombic, or monoclinic) F becomes a *cubic* polynomial with respect to q^2 , and its roots, along with the derivatives $q_{,i}$ and $q_{,ij}$, can be obtained explicitly. Equation (8) also represents a convenient tool for developing weak-anisotropy approximations for NMO velocity, which provide valuable insight into the influence of the anisotropic parameters on normal moveout (Tsvankin, 1995; Cohen, 1997).

Thus, equation (8) provides a simple and numerically efficient recipe to obtain azimuthally-dependent reflection moveout in an arbitrary anisotropic layer. Figure 1 illustrates the high accuracy of the hyperbolic moveout equation parameterized by the analytic NMO velocity (8) in describing conventional-spread reflection travel-times in an orthorhombic layer above a dipping reflector. Despite the presence of anisotropy-induced nonhyperbolic moveout, the P -wave NMO velocity is close to the moveout (stacking) velocity calculated from the exact traveltimes on six CMP lines with different orientation. The maximum difference between V_{nmo} (solid line) and the finite-spread moveout velocity (dots) is just 1.4%, which is even less than the corresponding value (2.7%) for the same model, but with a *horizontal* reflector (see

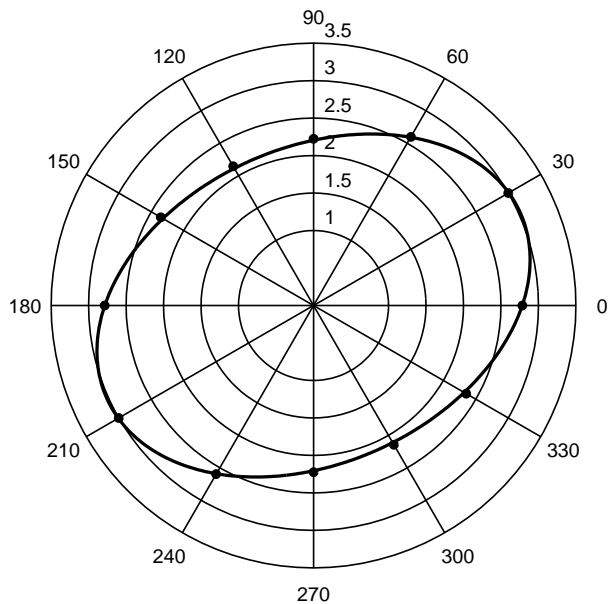


FIG. 1. Comparison of the P -wave NMO velocity from equation (8) (solid line) and the moveout (stacking) velocity (dots) obtained by least-squares fitting of a hyperbola to the exact traveltimes computed for speedlength equal to the reflector depth. The model contains a homogeneous orthorhombic layer (with the vertical symmetry planes at azimuths 0° and 90°) above a plane dipping reflector; the dip and azimuth of the reflector are equal to 30° . The relevant medium parameters [in Tsvankin's (1996) notation] are $V_{P0} = 2.0$ km/s, $\epsilon^{(1)} = 0.110$, $\delta^{(1)} = -0.035$, $\epsilon^{(2)} = 0.225$, $\delta^{(2)} = 0.100$, $\delta^{(3)} = 0$. The vertical symmetry plane at zero azimuth has the properties of the VTI model of Dog Creek shale, while the second vertical symmetry plane is equivalent to Taylor sandstone; both models are described in Thomsen (1986).

Grechka and Tsvankin, 1996). Therefore, the magnitude of nonhyperbolic move-out for this model decreases with reflector dip; the same observation was made by Tsvankin (1995) for vertical transverse isotropy. Note that although the azimuth of the dip plane of the reflector is equal to 30° , the largest axis of the $V_{\text{nmo}}(\alpha)$ ellipse has an azimuth of 24.3° due to the influence of the azimuthal anisotropy above the reflector.

Model with a vertical symmetry plane

Next, let us consider a special case – a model in which the dip plane of the reflector coincides with a vertical symmetry plane of the layer. The mirror symmetry with respect to the dip plane implies that one of the axes of the NMO ellipse points in the dip direction. Below, we provide a formal proof of this fact, as well as concise expressions for the azimuthally dependent NMO velocity in this model.

It is convenient to align the x_1 -axis with the azimuth of the dip plane, while the x_2 -axis will point in the strike direction. Evidently, the zero-offset ray should lie in the vertical symmetry plane [$x_2 = 0$], and its slowness component p_2 goes to zero. As another consequence of the mirror symmetry with respect to the dip plane, $\partial x_2 / \partial p_1 = 0$ (i.e, a change in p_1 cannot make a ray deviate from the dip plane [$x_2 = 0$]), so the matrix \mathbf{Y} from equation (B-6) becomes *diagonal*. Therefore, the cross-term q_{12} in equation (8) vanishes, and the NMO velocity simplifies to

$$V_{\text{nmo}}^2(\alpha, p_1) = \frac{q_{11}q_{22}}{p_1q_{11} - q} \left[q_{22} \cos^2 \alpha + q_{11} \sin^2 \alpha \right]^{-1}. \quad (10)$$

Equation (10) describes an ellipse with the semi-axes in the dip and strike directions:

$$V_{\text{nmo}}^2(\alpha = 0, p_1) = \frac{q_{11}}{p_1q_{11} - q}, \quad (11)$$

$$V_{\text{nmo}}^2(\alpha = \frac{\pi}{2}, p_1) = \frac{q_{22}}{p_1q_{11} - q}. \quad (12)$$

The dip-line NMO velocity (11) was originally derived via the derivatives of the in-plane phase velocity with respect to the phase angle by Tsvankin (1995); in the form (11) it was obtained by Cohen (1997). Equation (12) provides a similar representation for the NMO velocity in the strike direction.

Equations (11) and (12) are always valid for transversely isotropic media with a vertical symmetry axis because of the mirror symmetry with respect to *any* vertical plane in this model. The vertical slowness in VTI media can be represented as $q(p_1, p_2) \equiv q \left(\sqrt{p_1^2 + p_2^2} \right)$ and, for $p_2 = 0$, $q_{22} = q_{11}/p_1$. Then equation (12) for the strike-line NMO velocity reduces to the expression obtained previously by Grechka and Tsvankin (1996),

$$V_{\text{nmo}}^2(\alpha = \frac{\pi}{2}, p_1) = \frac{q_{11}}{p_1(p_1q_{11} - q)}. \quad (13)$$

Grechka and Tsvankin (1996) also gave an equivalent form of equation (13) in terms of the phase-velocity function and its weak-anisotropy approximation. Due to the axial symmetry of the VTI model, both the dip-line [equation (11)] and strike-line [equation (13)] NMO velocities depend on the derivatives of q with respect to the single horizontal (in-plane) slowness component (p_1). The cubic equation for $q^2(p_1)$ in VTI media is particularly easy to solve because it splits into a quadratic equation for $P - SV$ waves and a linear equation for the SH -wave.

Finally, in isotropic media the vertical slowness can be directly expressed through the reflector dip ϕ :

$$q = \sqrt{V^{-2} - p_1^2} = \frac{\cos \phi}{V},$$

and equations (11) and (13) reduce to the well-known relationships given by Levin (1971):

$$V_{\text{nmo}}(\alpha = 0) = \frac{V}{\cos \phi}, \quad (14)$$

$$V_{\text{nmo}}(\alpha = \frac{\pi}{2}) = V. \quad (15)$$

HORIZONTALLY-LAYERED MEDIUM ABOVE A DIPPING REFLECTOR

Generalized Dix equation

Here, we show that the NMO ellipse for vertically inhomogeneous arbitrary anisotropic media above a dipping reflector can be obtained by Dix-type averaging of the matrices \mathbf{W} responsible for the interval NMO ellipses. In our derivation we essentially follow the approach employed by Alkhalifah and Tsvankin (1995) to obtain their “2-D” Dix-type NMO equation for rays confined to the incidence (vertical) plane that contains the CMP line. Their equation is valid only in the dip plane of the reflector, which should also coincide with a symmetry plane of the medium. In contrast, we make no assumptions about the mutual orientation of the CMP line and reflector strike, and take full account of the out-of-plane phenomena associated with both model geometry and depth-varying anisotropy.

To construct the NMO ellipse, we need to obtain the matrix \mathbf{W} defined in equation (4):

$$W_{ij}(L) = \tau(L) \frac{\partial p_i}{\partial x_j(L)}, \quad (i, j = 1, 2), \quad (16)$$

where $\tau(L)$ is the total zero-offset traveltime and $x_i(L)$ is the horizontal ray displacement between the zero-offset reflection point located at the L -th (generally dipping) interface and the surface. Due to the continuity of the ray, both $\tau(L)$ and $x_i(L)$ are equal to the sum of the respective interval values:

$$\tau(L) = \sum_{\ell=1}^L \tau_{\ell}, \quad (17)$$

$$x_i(L) = \sum_{\ell=1}^L x_{i,\ell}, \quad (i = 1, 2). \quad (18)$$

(Note that here and below, the comma in the subscripts separates the layer index.)

It is convenient to introduce an auxiliary matrix

$$Y_{ij}(L) \equiv \frac{\partial x_i(L)}{\partial p_j}, \quad (i, j = 1, 2) \quad (19)$$

with derivatives evaluated for the ray parameters p_1 and p_2 of the zero-offset ray. Then

$$\mathbf{W} \equiv \mathbf{W}(L) = \tau(L) \mathbf{Y}^{-1}(L). \quad (20)$$

Our goal is to decompose the matrix \mathbf{W} into the contributions of the individual layers. In a model composed of horizontally homogeneous layers above the reflector, the horizontal components p_1 and p_2 of the slowness vector remain constant along any given ray between the reflection point and the surface. Therefore, substituting equation (18) into equation (19), we find

$$Y_{ij}(L) \equiv \frac{\partial x_i(L)}{\partial p_j} = \sum_{\ell=1}^L \frac{\partial x_{i,\ell}}{\partial p_j} \equiv \sum_{\ell=1}^L Y_{ij,\ell}. \quad (21)$$

Equation (21) explains the reason for introducing the effective matrix $\mathbf{Y}(L)$: unlike the matrix \mathbf{W} , it can be decomposed into the sum of the matrices \mathbf{Y}_ℓ for the individual layers. Since all interfaces are horizontal, in this model, the ray displacements $x_{i,\ell}$ in any layer coincide with the values that should be used in computing the matrix \mathbf{W} and the interval NMO velocity for this particular layer. Hence, we can apply equation (20) to layer ℓ :

$$\mathbf{W}_\ell = \tau_\ell \mathbf{Y}_\ell^{-1} \quad (22)$$

and, therefore,

$$\mathbf{Y}_\ell = \tau_\ell \mathbf{W}_\ell^{-1}. \quad (23)$$

Substituting equations (23) and (21) into equation (20) leads to the final result:

$$\mathbf{W}^{-1}(L) = \frac{1}{\tau(L)} \sum_{\ell=1}^L \tau_\ell \mathbf{W}_\ell^{-1}. \quad (24)$$

Interval matrices \mathbf{W}_ℓ in terms of the components of the slowness vector are given by equation (7), while the traveltimes τ_ℓ should be obtained from the kinematic ray tracing (i.e., by computing group velocity) of the zero-offset ray. Note that, since the eigenvalues of the matrices \mathbf{W}_ℓ and $\mathbf{W}(L)$ usually are positive (under the assumptions discussed in Grechka and Tsvankin, 1996), these matrices are nonsingular and, therefore, can be inverted.

Equation (24) performs Dix-type averaging of the interval matrices \mathbf{W}_ℓ to obtain the effective matrix $\mathbf{W}(L)$ and, therefore, the effective normal-moveout velocity

$V_{\text{nmo}}(\alpha, L)$. It should be emphasized that the interval NMO velocities $V_{\text{nmo},\ell}(\alpha)$ (or the interval matrices \mathbf{W}_ℓ) in equation (24) are computed for the horizontal components of the slowness vector of the zero-offset ray. (As follows from Snell's law, the slowness vector of the zero-offset ray is normal to the reflector at the reflection point.) This means that the interval NMO velocities in equation (24) correspond to the generally *non-existent* reflectors that are orthogonal to the slowness vector of the zero-offset ray in each layer.

Equation (24) can be rewritten explicitly in the Dix differentiation form:

$$\mathbf{W}_\ell^{-1} = \frac{\tau(\ell)\mathbf{W}^{-1}(\ell) - \tau(\ell - 1)\mathbf{W}^{-1}(\ell - 1)}{\tau(\ell) - \tau(\ell - 1)}. \quad (25)$$

Equations (24) and (25) generalize the Dix (1955) formula for horizontally-layered arbitrary anisotropic media above a dipping reflector. Formally, this extension looks relatively straightforward: the squared NMO velocities in the Dix formula are simply replaced by the inverse matrices \mathbf{W}^{-1} . In contrast to the conventional Dix equation, however, the effective matrix $\mathbf{W}^{-1}(\ell - 1)$ *cannot* be obtained directly from seismic data since the corresponding reflector usually does not exist in the subsurface. Therefore, layer-stripping by means of equation (25) involves recalculating each interval matrix \mathbf{W} from one value of the slowness vector (corresponding to a certain real reflector in a given layer) to another – that of the zero-offset ray. This procedure was discussed for the 2-D case by Alkhakifah and Tsvankin (1995) and further developed for P -waves in VTI media by Alkhalifah (1996); the latter paper also contains a successful application of this algorithm to field data.

Only in the simplest special case of a *horizontal* reflector, does the slowness vector of the zero-offset ray not change its direction (stays vertical) all the way to the surface, and the interval matrices \mathbf{W}_ℓ correspond to the NMO velocities from horizontal interfaces that can be measured from reflection data. Note that although such a model is horizontally-homogeneous, the zero-offset ray is not necessarily vertical, in anisotropic media, and the zero-offset reflection point may be shifted in the horizontal direction from the CMP location.

Model with a vertical symmetry plane

Next, we consider the same special case – a model in which all layers have a common vertical symmetry plane that coincides with the dip plane of the reflector. For such a medium the matrices \mathbf{W}_ℓ in the individual layers are diagonal (see the previous section), and

$$W_{12,\ell} = 0. \quad (26)$$

Consequently, the off-diagonal elements of the matrix $\mathbf{W}(L)$ [equation (24)] vanish as well:

$$W_{12}(L) = 0. \quad (27)$$

If the matrix \mathbf{W} is diagonal, its two components directly determine the semi-axes of the NMO ellipse (see equation (3) and Appendix A):

$$W_{kk,\ell} = [V_{\text{nmo},\ell}^{(k)}]^{-2} \quad (28)$$

and

$$W_{kk}(L) = [V_{\text{nmo}}^{(k)}(L)]^{-2}, \quad (k = 1, 2), \quad (29)$$

where $[V_{\text{nmo}}^{(1)} \equiv V_{\text{nmo}}(\alpha = 0)]$ and $[V_{\text{nmo}}^{(2)} \equiv V_{\text{nmo}}(\alpha = \pi/2)]$ are the NMO velocities measured in the dip and strike directions, respectively.

Substitution of equations (26) – (29) into equations (24) and (25) yields more conventional Dix-type averaging and differentiation formulas for the dip- and strike-components of the normal-moveout velocity:

$$[V_{\text{nmo}}^{(k)}(L)]^2 = \frac{1}{\tau(L)} \sum_{\ell=1}^L \tau_{\ell} [V_{\text{nmo},\ell}^{(k)}]^2 \quad (30)$$

and

$$[V_{\text{nmo},\ell}^{(k)}]^2 = \frac{\tau(\ell)[V_{\text{nmo}}^{(k)}(\ell)]^2 - \tau(\ell-1)[V_{\text{nmo}}^{(k)}(\ell-1)]^2}{\tau(\ell) - \tau(\ell-1)}, \quad (k = 1, 2). \quad (31)$$

Equations (30) and (31) for the *dip* component ($k = 1$) of the NMO velocity were derived by Alkhalifah and Tsvankin (1995) who considered 2-D wave propagation in the the dip plane of the reflector. Our derivation shows that the same Dix-type equations can be applied to the *strike*-component ($k = 2$) of the NMO velocity, which determines the second semi-axis of the NMO ellipse. Despite the close resemblance of expressions (30) and (31) to the conventional Dix equation, the interval NMO velocities in equations (30) and (31), as in the more general Dix equation discussed above, correspond to the *non-existent* reflectors normal to the slowness vector of the zero-offset ray in each layer.

Accuracy of the rms averaging of NMO velocities

Although the generalized Dix equation (24) operates with the *matrices* \mathbf{W}_{ℓ}^{-1} , we showed that Dix-type averaging can be applied to the dip- and strike-components of the *normal-moveout velocity* in a model that has a common (throughgoing) vertical symmetry plane aligned with the dip plane of the reflector. Here, we examine the accuracy of this more conventional averaging procedure at an *arbitrary* azimuth α in a model that may or may not have vertical symmetry planes. Using equation (3), we express the NMO velocity obtained by the Dix averaging of the interval velocities as

$$\begin{aligned} \tilde{V}_{\text{nmo}}^2(L, \alpha) &= \frac{1}{\tau(L)} \sum_{\ell=1}^L \tau_{\ell} V_{\text{nmo},\ell}^2(\alpha) \\ &= \frac{1}{\tau(L)} \sum_{\ell=1}^L \tau_{\ell} [W_{11,\ell} \cos^2 \alpha + 2 W_{12,\ell} \sin \alpha \cos \alpha + W_{22,\ell} \sin^2 \alpha]^{-1}. \end{aligned} \quad (32)$$

Note that all interval normal-moveout velocities in equation (32) are taken at the azimuth of the CMP line. In general, the velocity $\tilde{V}_{\text{nmo}}(L, \alpha)$, from equation (32) may be thought of as an approximation of the exact normal-moveout velocity $V_{\text{nmo}}(L, \alpha)$ expressed by equation (3),

$$V_{\text{nmo}}^2(L, \alpha) = \left[W_{11}(L) \cos^2 \alpha + 2 W_{12}(L) \sin \alpha \cos \alpha + W_{22}(L) \sin^2 \alpha \right]^{-1}, \quad (33)$$

where elements of the matrix $\mathbf{W}(L)$ are given by the generalized Dix equation (24). Clearly, the averaging of the inverse interval matrices \mathbf{W}_ℓ^{-1} in equation (24) is different from the rms averaging of the interval velocities $V_{\text{nmo},\ell}(\alpha)$ in equation (32). While the exact NMO velocity $V_{\text{nmo}}(L, \alpha)$ from equation (33) is an ellipse in the horizontal plane, the approximate velocity $\tilde{V}_{\text{nmo}}(L, \alpha)$ [equation (32)] is a smooth oval curve that does not necessarily have an elliptical shape. Nevertheless, even for general anisotropic media the two curves may be close to each other if the interval $V_{\text{nmo},\ell}(\alpha)$ ellipses are not far different from circles. As shown in Appendix C, if the eigenvalues $\lambda_{1,\ell}$ and $\lambda_{2,\ell}$ of the matrices \mathbf{W}_ℓ are written as

$$\lambda_{\text{max},\ell} = \lambda_{\text{min},\ell} (1 + \mu_\ell) \quad (34)$$

where $\lambda_{\text{max},\ell}$ are the larger eigenvalues, then the NMO velocity $\tilde{V}_{\text{nmo}}(L, \alpha)$ gives a linear approximation to the exact velocity $V_{\text{nmo}}(L, \alpha)$:

$$V_{\text{nmo}}(L, \alpha) = \tilde{V}_{\text{nmo}}(L, \alpha) + O(\mu^2) \quad (35)$$

for any azimuth α . Here, μ is defined by

$$\mu_\ell < \mu \ll 1 \quad (\text{for all } \ell). \quad (36)$$

Equation (35) and inequality (36) show that the rms averaging of the interval NMO velocities is sufficiently accurate if the combined influence of azimuthal anisotropy and reflector dip on the interval velocities $V_{\text{nmo},\ell}(\alpha)$ is weak in the sense of condition (36). It is important to emphasize that both azimuthal anisotropy and reflector dip influence the NMO velocity in a similar way: they make the interval NMO ellipses elongated, pulling them away from a circular shape.

In order to study the accuracy of equation (32), we consider several numerical examples. Figure 2 shows the azimuthally-dependent P -wave NMO velocity in an orthorhombic medium consisting of three horizontal layers with moderate azimuthal anisotropy (10% of azimuthal NMO velocity variation in the first and third layers and 20% in the second layer). Evidently, the rms averaging of the interval normal-moveout velocities using equation (32) gives an excellent approximation to the exact NMO-velocity ellipse with a maximum error of just 0.76%. Even though the values of μ_ℓ are not that small ($\mu_1 = \mu_3 = 0.18$ and $\mu_2 = 0.50$), the quadratic terms in μ_ℓ in equation (35) are not large enough to cause noticeable errors in the rms averaging of NMO velocities.

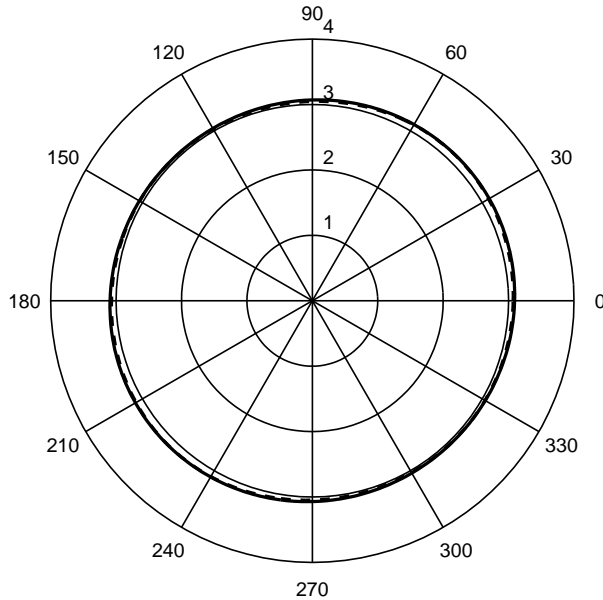


FIG. 2. Comparison of the exact P -wave NMO ellipse from equation (33) (solid line) and an approximate NMO velocity obtained by the Dix-type averaging [equation (32), dashed line]. The model contains three horizontal orthorhombic layers with a horizontal ($[x_1, x_2]$) symmetry plane. The azimuth of the $[x_1, x_3]$ symmetry plane (also, the direction of one of the axes of the interval NMO ellipse) in the first (subsurface) layer is $\beta_1 = 0^\circ$, in the second layer - $\beta_2 = 45^\circ$, and in the third layer - $\beta_3 = 60^\circ$; (azimuthal angles are shown along the perimeter of the plot). The vertical P -wave velocities are $V_{P0,1} = 2.0$ km/s, $V_{P0,2} = 3.0$ km/s, and $V_{P0,3} = 3.5$ km/s; the interval zero-offset traveltimes are equal to each other ($\tau_1 = \tau_2 = \tau_3 = 1.0$ s). The relevant anisotropic parameters [in Tsvankin's (1996) notation] are: Layer 1 - $\delta_1^{(1)} = 0.15$, $\delta_1^{(2)} = 0.05$; Layer 2 - $\delta_2^{(1)} = -0.10$, $\delta_2^{(2)} = 0.10$; Layer 3 - $\delta_3^{(1)} = 0.15$, $\delta_3^{(2)} = 0.05$.

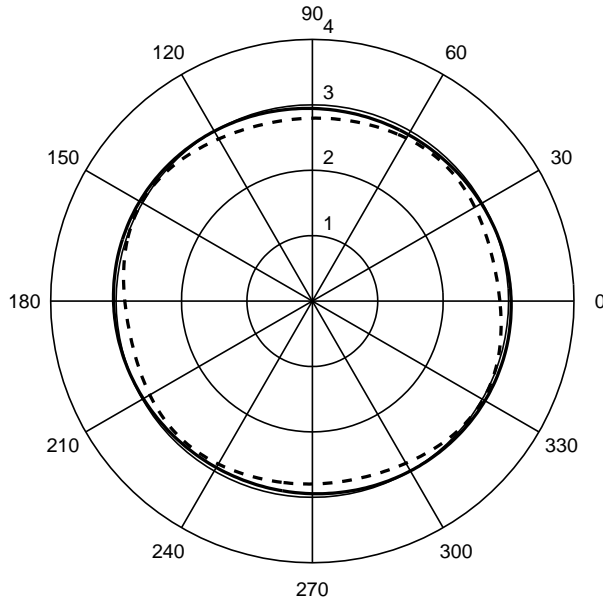


FIG. 3. The exact P -wave NMO ellipse given by equation (33) (solid line) and the approximation from equation (32) (dashed line) in an orthorhombic model similar to that in Figure 2 but with the anisotropic parameters $\delta_1^{(1)} = 0.25$, $\delta_1^{(2)} = -0.15$, $\delta_2^{(1)} = -0.20$, $\delta_2^{(2)} = 0.20$, $\delta_3^{(1)} = 0.25$, and $\delta_3^{(2)} = -0.15$.

In contrast, for the model in Figure 3 equation (32) is substantially less accurate. In this case, the azimuthal variation in the interval NMO velocity is much stronger (about 40% in all layers), and the condition (36) is clearly violated ($\mu_1 = \mu_3 = 1.14$ and $\mu_2 = 1.33$). While the exact NMO ellipse (solid line) happens to be close to a circle, the approximate normal-moveout velocity (dashed line) has an oval noncircular shape because the interval NMO ellipses are far different from circles. The maximum error of the approximation (32) is about 6.3%, which will lead to much higher errors in the interval velocities after application of the Dix differentiation (31). Evidently, for this model it is necessary to use the exact NMO equation (33), which properly accounts for the influence of azimuthal anisotropy on normal moveout.

The strength of P -wave azimuthal anisotropy, however, seldom reaches the level used in the model from Figure 3. Therefore the Dix rms averaging of the interval NMO velocities produces sufficiently accurate results for horizontal reflections in vertically inhomogeneous models with moderate azimuthal velocity variations. The same conclusion was drawn by Al-Dajani and Tsvankin (1996) in their study of normal moveout in layered transversely isotropic models with a horizontal symmetry axis (HTI media). Equation (32) works especially well in the presence of a common (throughgoing) vertical symmetry plane because in this case the rms averaging of the NMO velocities is exact in the directions of both axes of the NMO ellipse.

Another example, in which the interval NMO ellipses differ from circles due to the influence of reflector dip in a purely *isotropic* layered model, is shown in Figure 4.

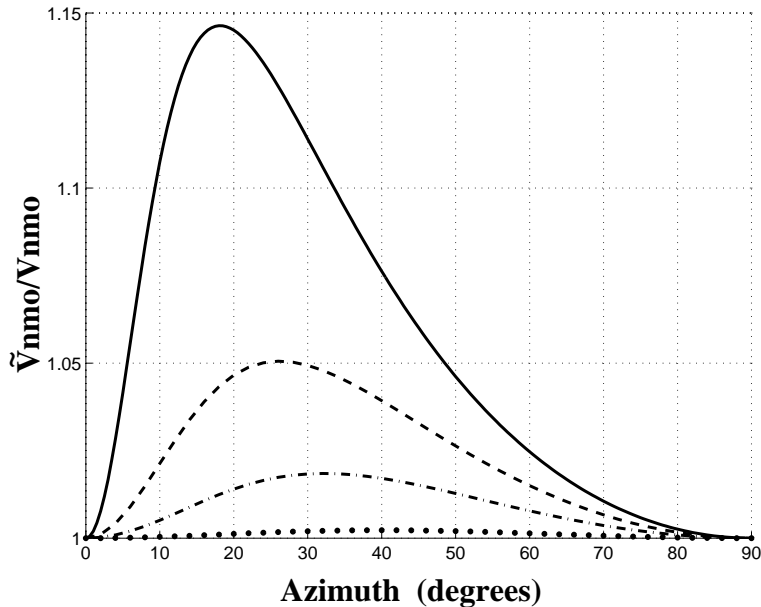


FIG. 4. The ratio $\tilde{V}_{\text{nmo}}/V_{\text{nmo}}$ calculated from equations (32) and (33) in *isotropic* media as a function of the azimuth of the CMP line with respect to the dip plane of the reflector. The model contains three layers above the reflector with the interval velocities $V_1 = 2.0$ km/s, $V_2 = 3.0$ km/s, and $V_2 = 3.5$ km/s and the interval zero-offset traveltimes $\tau_1 = \tau_2 = \tau_3 = 1.0$ s. The reflector dips are $\phi = 40^\circ$ (dotted line), $\phi = 60^\circ$ (dashed-dotted line), $\phi = 70^\circ$ (dashed line), and $\phi = 80^\circ$ (solid line).

Obviously, in this model the dip plane of the reflector always represents a symmetry plane, and one of the axes of all interval NMO ellipses is parallel to the dip direction. As shown in the previous section, in this case the rms averaging of the interval NMO velocities [equations (30) or (32)] becomes exact for the dip (azimuth $\alpha = 0^\circ$) and strike CMP lines (azimuth $\alpha = 90^\circ$), where the interval NMO values are well known [e.g., Levin (1971)]. Figure 4 corroborates this conclusion: for azimuths $\alpha = 0^\circ$ and $\alpha = 90^\circ$ the ratio $\tilde{V}_{\text{nmo}}/V_{\text{nmo}} = 1$. In all other azimuths, equation (32) gives only an approximation to the exact NMO velocity. However, Figure 4 indicates that this approximation is quite accurate for small and moderate reflector dips. The maximum error of equation (32), for example, is only 0.22% for reflector dip $\phi = 40^\circ$ and 1.85% for dip $\phi = 60^\circ$. Clearly, the error increases with dip because the interval NMO ellipses become more elongated and diverge more from a circle.

Again, since the reflector is dipping, the interval NMO velocities here are calculated for the nonzero horizontal components of the slowness vector determined by the reflector dip. These interval velocities correspond to non-existent reflectors and need to be recalculated from the NMO velocities of the horizontal events (which is, however, straightforward for isotropic media).

INHOMOGENEOUS ANISOTROPIC MEDIA

Summary of ray tracing

Here, we give an overview of ray-theory equations for anisotropic media (e.g., Červený, 1972; Červený, Molotkov, and Pšenčík, 1977; Kendall and Thomson, 1989) needed for our further derivations. The wave equation in anisotropic inhomogeneous media can be written in the frequency domain as

$$\rho\omega^2 u_i + \frac{\partial}{\partial x_j} \left(c_{ijkl} \frac{\partial u_l}{\partial x_k} \right) = 0, \quad (37)$$

where ω is the angular frequency, $\rho \equiv \rho(\mathbf{x})$ is the density, $c_{ijkl} \equiv c_{ijkl}(\mathbf{x}) = \rho(\mathbf{x})a_{ijkl}(\mathbf{x})$ is the elasticity tensor in the Cartesian coordinates \mathbf{x} , and $\mathbf{u} \equiv \mathbf{u}(\mathbf{x})$ is the displacement vector. The indices i, j, k, l take on values from 1 to 3; summation over repeated indices is implied.

Within the framework of ray theory, the displacement field is sought in the form of a series expansion,

$$\mathbf{u}(\mathbf{x}, \omega) = \sum_{n=0}^{\infty} \frac{\mathbf{U}^{(n)}(\mathbf{x})}{(-i\omega)^n} \exp^{i\omega\tau(\mathbf{x})}. \quad (38)$$

Substituting this trial solution into equation (37) and retaining only the leading (zeroth-order) term of the series (38) yields

$$(a_{ijkl} p_j p_k - \delta_{il}) A_l = 0, \quad (39)$$

where $\mathbf{A} \equiv \mathbf{U}^{(0)}$, $p_j \equiv p_j(\mathbf{x}) = \partial\tau/\partial x_j$ is the slowness vector, δ_{il} is the symbolic Kronecker delta, and \mathbf{A} is the polarization vector. Note that the slowness vector \mathbf{p} is normal to the wavefront $\tau(\mathbf{x}) = \text{constant}$. From equation (39) it is clear that a non-trivial (non-zero) solution for the vector \mathbf{A} exists only if the following (Christoffel) equation is satisfied:

$$F(\mathbf{p}) \equiv \det(a_{ijkl} p_j p_k - \delta_{il}) = 0. \quad (40)$$

For real quantities p_j corresponding to homogeneous waves, solutions $\mathbf{A}^{(r)}$ ($r = 1, 2, 3$) of equation (39) are real and orthogonal to each other. Therefore, they can be used to form an orthonormal basis:

$$\mathbf{A}^{(r)} \cdot \mathbf{A}^{(s)} = \delta_{rs}. \quad (41)$$

Since $p_j = \partial\tau/\partial x_j$ depends on \mathbf{x} in heterogeneous media, equation (39) can be regarded as a non-linear partial differential equation for the function $\tau(\mathbf{x})$. The Hamilton-Jacobi theory — or method of characteristics (Courant and Hilbert, 1962) — can be used to rewrite this equation in the form of the ordinary differential equations (the so-called “ray” equations):

$$\frac{dx_m}{d\tau} = \frac{1}{2} \frac{\partial H}{\partial p_m} = a_{imkl} A_i p_k A_l,$$

$$\frac{dp_m}{d\tau} = -\frac{1}{2} \frac{\partial H}{\partial x_m} = -\frac{1}{2} \frac{\partial a_{ijkl}}{\partial x_m} A_i p_j p_k A_l, \quad (m = 1, 2, 3). \quad (42)$$

The Hamiltonian H , obtained from equation (39), is given by

$$H \equiv H(\mathbf{p}, \mathbf{x}) = a_{ijkl} A_i p_j p_k A_l = 1. \quad (43)$$

Note that the first of equations (42) defines the group velocity,

$$\mathbf{g} \equiv \frac{d\mathbf{x}}{d\tau}. \quad (44)$$

Substituting the first equation (42) and equation (44) into (43), we obtain an important relation between the slowness and the group velocity vectors

$$\mathbf{p} \cdot \mathbf{g} = 1. \quad (45)$$

Since $\mathbf{p} = \mathbf{n}/V$, where \mathbf{n} is the unit vector in the phase (slowness) direction, and V is the phase velocity, equation (45) can be further rewritten as a relation between phase and group velocities,

$$\mathbf{n} \cdot \mathbf{g} = V. \quad (46)$$

For rays emanating from a point source located at the origin of the coordinate system, the ray-tracing equations (42) should be supplemented by the following initial conditions:

$$\mathbf{x}^{(0)} = \mathbf{0}, \quad \mathbf{p}^{(0)} = \frac{\mathbf{n}^{(0)}}{V^{(0)}}. \quad (47)$$

The ray-tracing system (42) combined with the initial conditions (47) can be solved by numerical integration using, for instance, the Runge-Kutta method.

Computation of NMO velocity

The results of Grechka and Tsvankin (1996), briefly reviewed above, show that there is no need to perform a full-scale multi-azimuth ray tracing to compute reflection traveltimes on conventional CMP spreads. It is clear from equation (3) that the NMO ellipse (6) and conventional-spread moveout as a whole are fully defined by only three quantities – W_{11} , W_{12} , and W_{22} . Thus, three well-separated azimuthal measurements of $V_{\text{nmo}}(\alpha)$ [which usually can be obtained using hyperbolic semblance analysis based on equation (1)] are sufficient to reconstruct the NMO ellipse and find the NMO velocity for any azimuth α . In practice, the values of $V_{\text{nmo}}(\alpha)$ determined on finite CMP spreads may be distorted by the influence of nonhyperbolic moveout. However, reflection moveout (especially that of P -waves) for spreadlengths close to the distance of the CMP from the reflector is typically close to hyperbolic; this has been shown in a number of publications (Tsvankin and Thomsen, 1994; Tsvankin, 1995; Grechka and Tsvankin, 1996) and is further illustrated by a numerical example in this work.

Although calculation of W_{ij} from $V_{\text{nmo}}(\alpha)$ obtained in three azimuths is much more efficient than multi-azimuth ray tracing, it still requires a considerable amount of computation and does not take advantage of the explicit expressions for the parameters of the NMO-velocity ellipse discussed above. It is much more attractive to build the NMO ellipse directly from equations (3) and (4), which requires obtaining the spatial derivatives of the ray parameter $\partial p_i/\partial x_j$ at the CMP location (i.e., for the zero-offset ray). Here, we outline an efficient method of calculating these derivatives based on the dynamic ray-tracing equations for the zero-offset ray.

Let us consider the zero-offset ray in the ray coordinates $(\gamma_1, \gamma_2, \tau)$. The parameter τ has the meaning of the traveltime along the ray, while γ_1 and γ_2 are supposed to uniquely determine the raypath and can be chosen, for instance, as the horizontal components of the slowness vector (p_1 and p_2). Here, we use another option suggested by Kashtan (1982) and Kendall and Thomson (1989), and define γ_1 and γ_2 as the polar and azimuthal angles of the slowness (wave-normal) vector (respectively):

$$\mathbf{n} = (\sin \gamma_1 \cos \gamma_2, \sin \gamma_1 \sin \gamma_2, \cos \gamma_1). \quad (48)$$

The derivatives $\partial p_i/\partial x_j$, needed to calculate $V_{\text{nmo}}(\alpha)$, can be formally written as

$$\frac{\partial p_i}{\partial x_j} = \frac{\partial p_i}{\partial \gamma_1} \frac{\partial \gamma_1}{\partial x_j} + \frac{\partial p_i}{\partial \gamma_2} \frac{\partial \gamma_2}{\partial x_j} + \frac{\partial p_i}{\partial \tau} \frac{\partial \tau}{\partial x_j}. \quad (49)$$

Using the matrix notation

$$\mathbf{P} = \left[\frac{\partial \mathbf{p}}{\partial \gamma_1}, \frac{\partial \mathbf{p}}{\partial \gamma_2}, \frac{\partial \mathbf{p}}{\partial \tau} \right], \quad \mathbf{X} = \left[\frac{\partial \mathbf{x}}{\partial \gamma_1}, \frac{\partial \mathbf{x}}{\partial \gamma_2}, \frac{\partial \mathbf{x}}{\partial \tau} \right] \quad (50)$$

and the fact that the inverse matrix \mathbf{X}^{-1} contains the rows

$$\mathbf{X}^{-1} = \begin{bmatrix} \partial \gamma_1 / \partial \mathbf{x} \\ \partial \gamma_2 / \partial \mathbf{x} \\ \partial \tau / \partial \mathbf{x} \end{bmatrix},$$

we represent equation (49) in the form

$$\frac{\partial p_i}{\partial x_j} = \mathbf{P} \mathbf{X}^{-1}. \quad (51)$$

Hence, if the matrices (50) have been calculated for the zero-offset ray at the CMP (surface) location, the derivatives $\partial p_i/\partial x_j$, ($i, j = 1, 2$) can be determined as the upper-left 2×2 submatrix of the 3×3 matrix (51). After computing the zero-offset traveltime τ_0 using kinematic ray tracing, we can find the NMO velocity from equations (3) and (4). Note that the values of $\partial p_i/\partial x_j$ used in the NMO-velocity calculation correspond to one-way propagation from the zero-offset reflection point to the surface (Grechka and Tsvankin, 1996). In other words, both \mathbf{p} and \mathbf{x} should

be computed for rays emanating from an imaginary source located at the reflection point of the zero-offset ray.

The third column of the matrices \mathbf{P} and \mathbf{X} [i.e. the derivatives $\partial\mathbf{p}/\partial\tau$ and $\partial\mathbf{x}/\partial\tau$] can be obtained using the kinematic ray-tracing equations (42). To find the first and second columns [i.e., the derivatives $\partial\mathbf{p}/\partial\gamma_n$ and $\partial\mathbf{x}/\partial\gamma_n$, ($n = 1, 2$)], let us consider the so-called dynamic ray-tracing equations responsible for the geometrical spreading along the ray (e.g., Červený, Molotkov and Pšenčík, 1977; Kendall and Thomson, 1989). These equations are obtained by differentiating the kinematic ray-tracing system (42) with respect to γ_1 and γ_2 .

$$\frac{d}{d\tau} \left(\frac{\partial x_m}{\partial \gamma_n} \right) = \frac{\partial}{\partial \gamma_n} (a_{imkl} A_i p_k A_l), \quad (52)$$

$$\frac{d}{d\tau} \left(\frac{\partial p_m}{\partial \gamma_n} \right) = -\frac{1}{2} \frac{\partial}{\partial \gamma_n} \left(\frac{\partial a_{ijkl}}{\partial x_m} A_i p_j p_k A_l \right), \quad (n = 1, 2; m = 1, 2, 3).$$

The initial conditions for these equations are, in turn, derived by differentiating the corresponding initial conditions (47) for the kinematic ray-tracing equations (42). Taking into account equation (46), we find

$$\begin{aligned} \frac{\partial \mathbf{x}^{(0)}}{\partial \gamma_n} &= \mathbf{0}, \\ \frac{\partial \mathbf{p}^{(0)}}{\partial \gamma_n} &= \frac{1}{V^{(0)}} \left[\frac{\partial \mathbf{n}^{(0)}}{\partial \gamma_n} - \frac{\mathbf{n}^{(0)}}{V^{(0)}} \left(\mathbf{g}^{(0)} \cdot \frac{\partial \mathbf{n}^{(0)}}{\partial \gamma_n} \right) \right], \quad (n = 1, 2), \end{aligned} \quad (53)$$

where $V^{(0)}$, $\mathbf{n}^{(0)}$, and $\mathbf{g}^{(0)}$ are the phase velocity, the unit vector in the wave-normal (phase) direction and the group-velocity vector at the source location. In our case, the velocities $V^{(0)}$ and $\mathbf{g}^{(0)}$ should be evaluated immediately above the reflector at the zero-offset reflection point (the effective source). The derivatives of the wave-normal vector $\partial\mathbf{n}^{(0)}/\partial\gamma_n$ can be computed in a straightforward way from equation (48).

Thus, the derivatives needed to obtain the normal-moveout velocity are exactly the same as those required to compute geometrical spreading. Therefore, the azimuthally-dependent NMO velocity in inhomogeneous arbitrary anisotropic media can be computed by integrating the dynamic ray-tracing equations (52) for the one-way zero-offset ray and substituting the results into equations (51), (4) and (3). Since this approach requires tracing of only *one* zero-offset ray together with the derivatives (52), it is orders of magnitude less time consuming than is the tracing of hundreds of reflected rays for different azimuths and source-receiver offsets as would otherwise be required. Moreover, as shown in the next section, our algorithm becomes significantly simpler, both analytically and computationally, if the model consists of homogeneous layers or blocks.

Piecewise homogeneous media

Let us consider a medium composed of arbitrary anisotropic *homogeneous* layers (or blocks) separated by smooth interfaces. In this case, the ray trajectory is piecewise linear, and integration of the kinematic ray-tracing equations (42) reduces to summation along straight ray segments:

$$\begin{aligned}\mathbf{x}^{(\ell)} &= \mathbf{x}^{(\ell-1)} + \mathbf{g}^{(\ell)} \tau^{(\ell)}, \\ \mathbf{p}^{(\ell)} &= \text{const},\end{aligned}\tag{54}$$

where $\mathbf{x}^{(\ell-1)}$ denotes the ray coordinate at the interface between the $\ell - 1$ -th and ℓ -th layer, $\tau^{(\ell)}$ is the travelttime inside the ℓ -th layer, and $g^{(\ell)}$ is the group velocity in this layer. Differentiation of equations (54) yields two derivatives required in the computation of the NMO ellipse:

$$\partial \mathbf{x} / \partial \tau = \mathbf{g},\tag{55}$$

$$\partial \mathbf{p} / \partial \tau = 0,\tag{56}$$

with the group-velocity vector \mathbf{g} evaluated for the zero-offset ray at the CMP location.

To fully describe the raypath (for purposes of kinematic ray tracing), equations (54) must be supplemented by the boundary conditions at model interfaces for \mathbf{x} and \mathbf{p} . The boundary conditions will also be used in the equations for dynamic ray tracing discussed below. Since the ray has to be continuous,

$$\mathbf{x}^{(\ell)} = \mathbf{x}^{(\ell-1)}.\tag{57}$$

The ray parameter \mathbf{p} satisfies Snell's law,

$$\mathbf{p}^{(\ell)} \times \mathbf{b}^{(\ell)} = \mathbf{p}^{(\ell-1)} \times \mathbf{b}^{(\ell)},\tag{58}$$

where “ \times ” denotes the cross product and $\mathbf{b}^{(\ell)}$ is the unit vector normal to the ℓ -th interface at $\mathbf{x}^{(\ell)}$.

Integration of the dynamic ray-tracing equations (52) in the case of homogeneous layers is relatively straightforward as well. Continuation of the derivatives $\partial \mathbf{x} / \partial \gamma_n$ and $\partial \mathbf{p} / \partial \gamma_n$ across the ℓ -th layer is expressed by

$$\frac{\partial \mathbf{x}^{(\ell+1)}}{\partial \gamma_n} = \frac{\partial \mathbf{x}^{(\ell)}}{\partial \gamma_n} + \frac{\partial \mathbf{g}^{(\ell+1)}}{\partial \gamma_n} \tau^{(\ell+1)}\tag{59}$$

and

$$\frac{\partial \mathbf{p}^{(\ell+1)}}{\partial \gamma_n} = \frac{\partial \mathbf{p}^{(\ell)}}{\partial \gamma_n}, \quad (n = 1, 2).\tag{60}$$

The derivative of the group velocity needed in equation (59) is obtained in Appendix D from equations (44) and (42).

To propagate the derivatives $\partial\mathbf{x}/\partial\gamma_n$ and $\partial\mathbf{p}/\partial\gamma_n$ across the ℓ -th (smooth) interface, Kashtan (1982) suggested differentiating equations (57) and Snell’s law [equation ((58))] with respect to γ_n . His results become especially simple for a plane interface with the normal $\mathbf{b}^{(\ell)}$:

$$\frac{\partial\mathbf{x}^{(\ell)}}{\partial\gamma_n} = \frac{\partial\mathbf{x}^{(\ell-1)}}{\partial\gamma_n} + \frac{\mathbf{g}^{(\ell)} - \mathbf{g}^{(\ell-1)}}{\mathbf{g}^{(\ell-1)} \cdot \mathbf{b}^{(\ell)}} \left(\mathbf{b}^{(\ell)} \cdot \frac{\partial\mathbf{x}^{(\ell-1)}}{\partial\gamma_n} \right) \quad (61)$$

and

$$\frac{\partial\mathbf{p}^{(\ell)}}{\partial\gamma_n} = \frac{\partial\mathbf{p}^{(\ell-1)}}{\partial\gamma_n} - \frac{\mathbf{b}^{(\ell)}}{\mathbf{b}^{(\ell)} \cdot \mathbf{g}^{(\ell)}} \left(\mathbf{g}^{(\ell)} \cdot \frac{\partial\mathbf{p}^{(\ell-1)}}{\partial\gamma_n} \right), \quad (n = 1, 2). \quad (62)$$

Equations (59) – (62) allow us to continue the initial values of the derivatives $\partial\mathbf{x}/\partial\gamma_n$ and $\partial\mathbf{p}/\partial\gamma_n$ [equations (53)] from the zero-offset reflection point through our layered (or blocked) model to the surface. Since the quantities needed to obtain these derivatives (i.e., the group velocity and traveltimes) have to be found for the kinematic ray-tracing anyway, the additional computational cost of this operation is minimal. Finally, we calculate the derivatives $\partial p_i/\partial x_j$ from equation (51) and construct the $V_{\text{nmo}}(\alpha)$ ellipse defined by equations (3) and (4).

The accuracy of this algorithm in modeling finite-spread reflection traveltimes in layered azimuthally anisotropic media is illustrated by Figure 5. The model contains two transversely isotropic layers with dipping lower boundaries and horizontal (but differently oriented) symmetry axes (HTI media). The P -wave NMO velocity calculated using the approach described above (solid line) is compared with the effective moveout velocity determined by least-square fitting of ray-traced traveltimes on a conventional spread equal to the distance between the CMP and the reflector (dots). The NMO ellipse is remarkably close to the effective moveout velocity for all four azimuths used in the computation, with the maximum difference of just about 0.4%. This test not only verifies the accuracy of our algorithm based on the evaluation of the derivatives $\partial\mathbf{x}/\partial\gamma_n$ and $\partial\mathbf{p}/\partial\gamma_n$, but also shows that the analytic (zero-spread) normal-moveout velocity provides an excellent approximation for P -wave reflection traveltimes on conventional spreads.

DISCUSSION AND CONCLUSIONS

For typical subsurface models, azimuthally-dependent normal-moveout velocity around a certain CMP location has an *elliptical* shape, with the orientation and semi-axes of the ellipse determined by the properties of the medium and the direction of the reflector normal at the zero-offset reflection point. Using this general result obtained by Grechka and Tsvankin (1996), we have presented a series of solutions for the exact normal-moveout velocity of pure modes in anisotropic models of various complexity. For a homogeneous anisotropic layer above a dipping reflector, NMO velocity was found explicitly as a function of the slowness vector corresponding to the zero-offset ray. This single-layer equation is valid for arbitrary anisotropic symmetry and any orientation of the CMP line with respect to the reflector strike. The vertical component

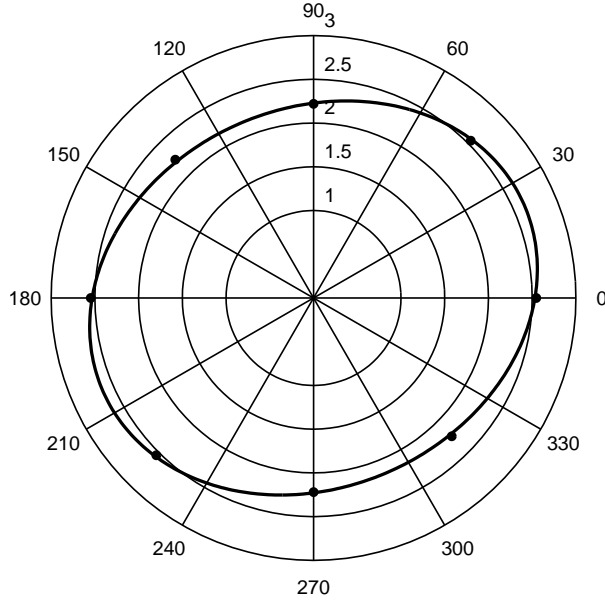


FIG. 5. Comparison of the P -wave NMO velocity and finite-spread moveout velocity in layered azimuthally-anisotropic media. The model consists of two dipping HTI layers with different azimuths of the symmetry axis (0° in the subsurface layer and 30° in the second one). The solid line is the $V_{\text{nmo}}(\alpha)$ ellipse computed from equations (3) and (4), with the spatial derivatives of the ray parameter evaluated using equations (51), (55), (56), and (59) through (62). The dots represent the effective moveout velocity found by least-squares fitting of ray-traced traveltimes on the spreadlength equal to the distance between the CMP and the reflector (the maximum offset is 2.0 km). The relevant model parameters [in Thomsen (1986) notation] are: $V_{P0,1} = 2.0$ km/s (the index “1” corresponds to the subsurface layer), $V_{P0,2} = 2.4$ km/s, $\epsilon_1 = \epsilon_2 = 0.0$, $\delta_1 = 0.2$, $\delta_2 = 0.1$. The dip ϕ and the azimuth ψ of the intermediate interface are $\phi_1 = 10^\circ$ and $\psi_1 = 70^\circ$. The dip and the azimuth of the reflector are $\phi_2 = 40^\circ$ and $\psi_2 = 20^\circ$. The distance between the CMP and the reflector is 2.0 km, between the CMP and the intermediate interface – 1 km.

of the slowness vector and its derivatives with respect to the horizontal slownesses, needed to compute the NMO velocity, can be obtained in a straightforward fashion from the Christoffel equation. If the medium has a horizontal symmetry plane (e.g., it can be TI, orthorhombic, or monoclinic), the Christoffel equation can be solved analytically and the NMO-velocity computation as a whole becomes an entirely analytic operation. In addition to simplifying moveout modeling, our NMO equation can be effectively used to develop weak-anisotropy approximations for different anisotropic symmetries. As demonstrated by the previous work for VTI and orthorhombic media (Tsvankin, 1995, 1996), these approximate solutions provide valuable insight into the dependence of normal moveout on the anisotropic coefficients.

If the model contains a stack of homogeneous arbitrary anisotropic layers above a dipping reflector, the NMO ellipse should be obtained by a Dix-type averaging of the single-layer expressions described above. Instead of the squared NMO velocities in the conventional Dix formula, our generalized equation operates with the interval matrices \mathbf{W}_ℓ that describe the NMO *ellipses* corresponding to the individual layers. Hence, to find azimuthally-dependent NMO velocity for this model, it is sufficient to compute the zero-offset traveltime and the interval NMO ellipses for the slowness vector of the zero-offset ray. The generalized Dix equation can be used to perform moveout-based layer stripping and interval parameter estimation in vertically inhomogeneous anisotropic models of any symmetry.

One important special case considered in detail is a model with the same (through-going) vertical symmetry plane in all layers that also coincides with the dip plane of the reflector (e.g., the medium above the reflector has VTI symmetry). Because of the mirror symmetry with respect to the dip plane, the axes of the NMO ellipse are aligned with the dip and strike directions of the reflector. The generalized Dix equation in such a model reduces to the rms averaging of the dip-line and strike-line NMO velocities in the individual layers (these averages determine the semi-axes of the NMO ellipse). This result represents a 3-D extension of the Dix-type equation developed by Alkhalifah and Tsvankin (1995) for normal moveout in the dip plane of the reflector. It should be emphasized, however, that in the case of a dipping reflector the NMO velocities in the individual layers have to be calculated for the slowness vector of the zero-offset ray and, therefore, cannot be directly measured from the data.

Except for the special case described above, the exact squared NMO velocity is not equal to the rms average of the interval values. If the conventional form of the Dix equation is applied in all azimuthal directions, the effective NMO velocity generally takes an oval *anelliptic* form that thus deviates from the exact NMO ellipse. Still, this deviation is relatively small if the interval NMO ellipses are close to being circles, which implies the absence of large dips and significant azimuthal anisotropy. For instance, normal moveout from a horizontal reflector in typical anisotropic models with moderate azimuthal velocity variations can be well described by the conventional Dix equation, provided the interval velocities take anisotropy into account.

Finally, we consider the most general inhomogeneous media and present an algorithm that leads to a dramatic reduction in the amount of computations needed to obtain the NMO velocity and conventional-spread reflection moveout. All information required to construct the NMO ellipse is contained in the results of the *dynamic* ray tracing of a single (zero-offset) ray. Specifically, the derivatives that determine the geometrical spreading along the zero-offset ray are sufficient for calculating the spatial derivatives of the slowness vector, which are responsible for NMO velocity. Although dynamic ray tracing requires solving an additional system of differential equations together with the kinematic ray-tracing equations, this algorithm is orders of magnitude more efficient than multi-offset, multi-azimuth ray tracing. Furthermore, if the model consists of homogeneous layers or blocks separated by smooth interfaces, all quantities needed to find the NMO ellipse can be computed during the kinematic tracing of the zero-offset ray. In this case, only a few simple additional computations yield the NMO velocity along with the zero-offset traveltimes.

The normal-moveout velocity discussed here is defined in the zero-spread limit and cannot account for nonhyperbolic moveout caused by anisotropy and inhomogeneity on finite-spread CMP gathers. Nevertheless, our numerical examples for various anisotropic models demonstrate that the hyperbolic moveout equation parameterized by NMO velocity provides excellent accuracy in the description of reflection moveout (especially that of *P*-waves) on conventional spreads close to the reflector depth. Therefore, our results can be efficiently used in traveltimes inversion and dip-moveout processing for arbitrary anisotropic media.

ACKNOWLEDGMENTS

We are grateful to members of A(nisotropy)-team of the Center for Wave Phenomena (CWP), Colorado School of Mines, for helpful discussions. Special thanks to Ken Larner and Andreas Rüger who reviewed the manuscript. The support for this work was provided by the members of the Consortium Project on Seismic Inverse Methods for Complex Structures at CWP and by the United States Department of Energy (project “Velocity Analysis, Parameter Estimation, and Constraints on Lithology for Transversely Isotropic Sediments” within the framework of the Advanced Computational Technology Initiative).

REFERENCES

- Al-Dajani, A., and Tsvankin, I., 1996, Nonhyperbolic reflection moveout for horizontal transverse isotropy: Research Report, Center for Wave Phenomena (CWP-219); also, submitted to *Geophysics*.
- Alkhalifah, T., 1996, Seismic data processing in vertically inhomogeneous TI media: CWP-176, submitted to *Geophysics*.
- Alkhalifah, T., and Tsvankin, I., 1995, Velocity analysis in transversely isotropic media: *Geophysics*, **60**, 1550–1566.

- Červený, 1972, Seismic rays and ray intensities in inhomogeneous anisotropic media: Geophys. J. Roy. astr. Soc., **29**, 1–13.
- Červený, V., Molotkov, I.A., and Pšenčík, I., 1977, Ray method in seismology: Univ. of Karlova.
- Cohen, J.K., 1997, A convenient expression for the NMO velocity function in terms of ray parameter: Geophysics, in print.
- Courant, R., and Hilbert, D., 1962, Methods of mathematical physics: Interscience, New York.
- Dix, C.H., 1955, Seismic velocities from surface measurements: Geophysics, **20**, 68–86.
- Gajewski, D., and Pšenčík, I., 1987, Computation of high-frequency seismic wavefields in 3-D laterally inhomogeneous anisotropic media: Geophys. J. R. Astr. Soc., **91**, 383–411.
- Grechka, V., and Tsvankin, I., 1996, 3-D description of normal moveout in anisotropic media, Geophysics, submitted.
- Hake, H., Helbig, K., and Mesdag, C. S., 1984, Three-term Taylor series for $t^2 - x^2$ curves over layered transversely isotropic ground: Geophys. Prosp., **32**, 828–850.
- Hale, D., Hill, N. R., and Stefani, J., 1992, Imaging salt with turning wave seismic waves: Geophysics, **57**, 1453–1462.
- Hubral, P., and Krey, T., 1980, Interval velocities from seismic reflection measurements: Soc. Expl. Geophys.
- Kashtan, B.M., 1982, Calculation of the geometrical spreading in piecewise homogeneous anisotropic media: Problems of dynamic theory of seismic wave propagation, **22**, 14–24 (in Russian).
- Kendall, J-M., and Thomson, C.J., 1989, A comment on the form of the geometrical spreading equations, with some examples of seismic ray tracing in inhomogeneous anisotropic media: Geophys. J. Internat., **99**, 401–413.
- Levin, F.K., 1971, Apparent velocity from dipping interface reflections: Geophysics, **36**, 510–516.
- Shah, P.M., 1973, Use of wavefront curvature to relate seismic data with subsurface parameters: Geophysics, **38**, 812–825.
- Thomsen, L., 1986, Weak elastic anisotropy: Geophysics, **51**, 1954–1966.
- Tsvankin, I., 1995, Normal moveout from dipping reflectors in anisotropic media: Geophysics, **60**, 268–284.
- Tsvankin, I., 1996, Effective parameters and P -wave velocity for azimuthally anisotropic media: 66th Ann. Internat. Mtg., Soc. Expl. Geophys., Expanded Abstracts.
- Tsvankin, I., 1997, Reflection moveout and parameter estimation for horizontal transverse isotropy: Geophysics, in print.
- Tsvankin, I., and Thomsen, L., 1994, Nonhyperbolic reflection moveout in anisotropic media: Geophysics, **59**, 1290–1304.

APPENDIX A: RELATION BETWEEN THE MATRIX \mathbf{W} AND THE NMO VELOCITY ELLIPSE

Azimuthally dependent normal-moveout velocity is described by equation (3) of the main text as a general second-order curve in the horizontal plane. The expression for $V_{\text{nmo}}(\alpha)$ can be simplified further by aligning the horizontal coordinate axes with the eigenvectors of the symmetric matrix \mathbf{W} (Grechka and Tsvankin, 1996). This rotation reduces equation (3) to

$$V_{\text{nmo}}^{-2}(\alpha) = \lambda_1 \cos^2(\alpha - \beta) + \lambda_2 \sin^2(\alpha - \beta), \quad (\text{A-1})$$

where λ_1 and λ_2 are the eigenvalues of the matrix \mathbf{W} , and β is the angle between the eigenvector corresponding to λ_1 and the x_1 -axis.

To verify the equivalence between equations (A-1) and (3), we expand

$$\cos^2(\alpha - \beta) = \cos^2 \alpha \cos^2 \beta + 2 \sin \alpha \sin \beta \cos \alpha \cos \beta + \sin^2 \alpha \sin^2 \beta$$

and

$$\sin^2(\alpha - \beta) = \cos^2 \alpha \sin^2 \beta - 2 \sin \alpha \sin \beta \cos \alpha \cos \beta + \sin^2 \alpha \cos^2 \beta.$$

Equations (A-1) and (3) are identical if

$$W_{11} = \lambda_1 \cos^2 \beta + \lambda_2 \sin^2 \beta, \quad (\text{A-2})$$

$$W_{12} = \frac{1}{2} (\lambda_1 - \lambda_2) \sin 2\beta, \quad (\text{A-3})$$

and

$$W_{22} = \lambda_1 \sin^2 \beta + \lambda_2 \cos^2 \beta. \quad (\text{A-4})$$

Inverting equations (A-2) – (A-4) for $\lambda_{1,2}$ and β yields

$$\lambda_{1,2} = \frac{1}{2} \left[W_{11} + W_{22} \pm \sqrt{(W_{11} - W_{22})^2 + 4W_{12}^2} \right] \quad (\text{A-5})$$

and

$$\tan \beta = \frac{W_{22} - W_{11} + \sqrt{(W_{22} - W_{11})^2 + 4W_{12}^2}}{2W_{12}}, \quad (W_{12} \neq 0). \quad (\text{A-6})$$

Equations (A-5) and (A-6) show that $\lambda_{1,2}$ are indeed the eigenvalues of \mathbf{W} and $\tan \beta$ is equal to the ratio of the components “2” and “1” of the eigenvector corresponding to λ_1 . If $W_{12} = 0$, the matrix \mathbf{W} is diagonal, and equation (3) reduces to equation (A-1) without any rotation.

As follows from equation (A-1), $V_{\text{nmo}}(\alpha)$ represents an ellipse in the horizontal plane if the eigenvalues $\lambda_{1,2}$ are positive (Grechka and Tsvankin, 1996). The “principal” values of the azimuthally dependent NMO velocity (the semi-axes of the ellipse) are given by

$$V_{\text{nmo}}^{(i)} = \frac{1}{\sqrt{\lambda_i}}, \quad (i = 1, 2). \quad (\text{A-7})$$

APPENDIX B: NMO VELOCITY IN A SINGLE LAYER

Here, we obtain the exact expression for the NMO velocity from a dipping reflector beneath a homogeneous arbitrary anisotropic layer. The derivation is based on the general equations (3) and (4) describing the NMO ellipse and follows the approach suggested for the 2-D case by Cohen (1997).

To evaluate the derivatives $\partial x_i / \partial p_j$, we have to relate the horizontal ray displacements (x_1, x_2) between the zero-offset reflection point and the surface to the horizontal components of the slowness vector (p_1, p_2) . We start by introducing the group-velocity vector \mathbf{g} ,

$$x_i = g_i \tau, \quad (i = 1, 2, 3), \quad (\text{B-1})$$

where τ is the one-way traveltime. Using the fact that the projection of the group-velocity vector on the slowness direction is equal to phase velocity [e.g., equation (45)], we can write

$$\mathbf{p} \cdot \mathbf{g} = p_1 g_1 + p_2 g_2 + p_3 g_3 = 1, \quad (\text{B-2})$$

Differentiating equation (B-2) with respect to p_i ($i = 1, 2$) and taking into account that the vertical slowness component p_3 can be considered as a function of p_1 and p_2 yields

$$g_i = -\frac{\partial p_3}{\partial p_i} g_3 - \mathbf{p} \cdot \frac{\partial \mathbf{g}}{\partial p_i}, \quad (i = 1, 2).$$

Since the slowness vector \mathbf{p} is normal to the group-velocity surface (wavefront) $\mathbf{g}(p_1, p_2)$, while the vectors $\partial \mathbf{g} / \partial p_i$ are tangent to this surface, $\mathbf{p} \cdot \frac{\partial \mathbf{g}}{\partial p_i} = 0$. Hence,

$$g_i = -q_{,i} g_3, \quad (i = 1, 2), \quad (\text{B-3})$$

where $q \equiv q(p_1, p_2) \equiv p_3$ denotes the vertical slowness, and $q_{,i} \equiv \partial q / \partial p_i$. Substitution of equations (B-3) into equation (B-2) gives a representation of the vertical group-velocity component that will be needed later in the derivation:

$$g_3 = \frac{1}{q - p_1 q_{,1} - p_2 q_{,2}}. \quad (\text{B-4})$$

Using equations (B-3), we rewrite the horizontal ray displacements x_i ($i = 1, 2$) from equations (B-1) as

$$x_i = -q_{,i} g_3 \tau, \quad (i = 1, 2). \quad (\text{B-5})$$

Note that $g_3 \tau$ is the depth of the zero-offset reflection point, which is independent of the slowness components (p_1, p_2) . Therefore, differentiating equations (B-5) gives

$$Y_{ij} \equiv \frac{\partial x_i}{\partial p_j} = -q_{,ij} g_3 \tau, \quad (\text{B-6})$$

where $q_{,ij} \equiv \partial^2 q / \partial p_i \partial p_j$ is a symmetric matrix of the second derivatives of the vertical slowness.

The NMO ellipse is determined by the matrix \mathbf{W} [equation (4)],

$$\mathbf{W} = \tau_0 \mathbf{Y}^{-1}, \quad (\text{B-7})$$

where the inverse matrix \mathbf{Y}^{-1} should be evaluated for the horizontal slowness components of the zero-offset ray.

Substituting Y_{ij} from equation (B-6) into equation (B-7) and using expression (B-4) for g_3 , we obtain

$$\mathbf{W} = \tau_0 \mathbf{Y}^{-1} = \frac{p_1 q_{,1} + p_2 q_{,2} - q}{q_{,11} q_{,22} - q_{,12}^2} \begin{pmatrix} q_{,22} & -q_{,12} \\ -q_{,12} & q_{,11} \end{pmatrix}, \quad (\text{B-8})$$

With the matrix \mathbf{W} from equation (B-8), equation (3) of the NMO ellipse in a homogeneous arbitrary anisotropic layer takes the following form:

$$\begin{aligned} V_{\text{nmo}}^2(\alpha) &\equiv V_{\text{nmo}}^2(\alpha, p_1, p_2) \\ &= \frac{q_{,11} q_{,22} - q_{,12}^2}{p_1 q_{,1} + p_2 q_{,2} - q} \left[q_{,22} \cos^2 \alpha - 2q_{,12} \sin \alpha \cos \alpha + q_{,11} \sin^2 \alpha \right]^{-1}. \end{aligned} \quad (\text{B-9})$$

APPENDIX C: RELATION BETWEEN THE EXACT AND RMS-AVERAGED NMO VELOCITY

Here, we examine the accuracy of the rms averaging of the interval NMO velocities for a model that consists of a stack of horizontal arbitrary anisotropic layers above a dipping reflector. The interval NMO velocity in the ℓ -th layer is expressed by equation (3):

$$V_{\text{nmo},\ell}^{-2}(\alpha) = W_{11,\ell} \cos^2 \alpha + 2 W_{12,\ell} \sin \alpha \cos \alpha + W_{22,\ell} \sin^2 \alpha. \quad (\text{C-1})$$

The symmetric matrix \mathbf{W}_ℓ is expressed through its eigenvalues $\lambda_{1,\ell}$ and $\lambda_{2,\ell}$ in equations (A-2) – (A-4). Here, we assume that $\lambda_{1,\ell} > \lambda_{2,\ell}$:

$$\begin{aligned} \lambda_{2,\ell} &\equiv \lambda_\ell, \\ \lambda_{1,\ell} &\equiv \lambda_\ell(1 + \mu_\ell), \end{aligned} \quad (\text{C-2})$$

and

$$\mu_\ell < \mu \ll 1,$$

for all ℓ .

An approximate NMO velocity obtained by rms averaging of the interval values is given by equation (32):

$$\tilde{V}_{\text{nmo}}^2(L, \alpha) = \frac{1}{\tau(L)} \sum_{\ell=1}^L \tau_\ell \left[W_{11,\ell} \cos^2 \alpha + 2 W_{12,\ell} \sin \alpha \cos \alpha + W_{22,\ell} \sin^2 \alpha \right]^{-1} \quad (\text{C-3})$$

Our goal is to compare equation (C-3) with the exact velocity [equation (33)],

$$\begin{aligned}
V_{\text{nmo}}^2(L, \alpha) &= \left[W_{11}(L) \cos^2 \alpha + 2 W_{12}(L) \sin \alpha \cos \alpha + W_{22}(L) \sin^2 \alpha \right]^{-1} \\
&= \left[W_{11}^{-1}(L) W_{22}^{-1}(L) - W_{12}^{-2}(L) \right] \\
&\quad \times \left[W_{22}^{-1}(L) \cos^2 \alpha - 2 W_{12}^{-1}(L) \sin \alpha \cos \alpha + W_{11}^{-1}(L) \sin^2 \alpha \right]^{-1},
\end{aligned} \tag{C-4}$$

where $W_{ij}^{-1}(L)$ are the elements of the inverse matrix $\mathbf{W}^{-1}(L)$ given by the Dix-type equation (24):

$$\mathbf{W}^{-1}(L) = \frac{1}{\tau(L)} \sum_{\ell=1}^L \tau_{\ell} \mathbf{W}_{\ell}^{-1}. \tag{C-5}$$

Clearly, the direct rms averaging of NMO velocities in equation (C-3) is different from the more complicated averaging of the inverse matrices \mathbf{W}_{ℓ}^{-1} [equation (C-5)] used to obtain the exact NMO velocity in equation (C-5). Nevertheless, we will show that the two representations of the NMO velocity become identical in the *linear* approximation with respect to μ_{ℓ} , i.e.,

$$\tilde{V}_{\text{nmo}}(L, \alpha) = V_{\text{nmo}}(L, \alpha) + O(\mu_{\ell}^2). \tag{C-6}$$

In the following derivation, we keep only terms independent of or linear in μ_{ℓ} . Combining equations (C-2) and (A-2) – (A-4) allows us to express the interval matrices \mathbf{W}_{ℓ} through the eigenvalue λ_{ℓ} and μ_{ℓ} ,

$$\begin{aligned}
W_{11,\ell} &= \lambda_{\ell} (1 + \mu_{\ell} \cos^2 \beta_{\ell}), \\
W_{12,\ell} &= \lambda_{\ell} \mu_{\ell} \sin \beta_{\ell} \cos \beta_{\ell}, \\
W_{22,\ell} &= \lambda_{\ell} (1 + \mu_{\ell} \sin^2 \beta_{\ell}),
\end{aligned} \tag{C-7}$$

where β_{ℓ} are the rotation angles of the interval NMO ellipses introduced in Appendix A.

Substituting equation (C-7) into equation (C-3), we find the following linearized (in μ_{ℓ}) expression for the rms-averaged NMO velocity:

$$\tilde{V}_{\text{nmo}}^2(L, \alpha) = \frac{1}{\tau(L)} \sum_{\ell=1}^L \frac{\tau_{\ell}}{\lambda_{\ell}} \left[1 - \mu_{\ell} \cos^2(\alpha - \beta_{\ell}) \right]. \tag{C-8}$$

Next, we need to evaluate the NMO ellipse [equation (C-5)] in the same approximation. Using equation (C-7) and dropping terms quadratic in μ_{ℓ} , we represent the inverse matrices \mathbf{W}_{ℓ}^{-1} as

$$\mathbf{W}_{\ell}^{-1} = \frac{1}{\lambda_{\ell}} \begin{pmatrix} 1 - \mu_{\ell} \cos^2 \beta_{\ell} & -\mu_{\ell} \sin \beta_{\ell} \cos \beta_{\ell} \\ -\mu_{\ell} \sin \beta_{\ell} \cos \beta_{\ell} & 1 - \mu_{\ell} \sin^2 \beta_{\ell} \end{pmatrix}. \tag{C-9}$$

After averaging the matrices (C-9) in accordance with equation (C-5) and substituting the result into equation (C-5), we obtain

$$V_{\text{nmo}}^2(L, \alpha) = \frac{1}{\tau(L)} \sum_{\ell=1}^L \frac{\tau_\ell}{\lambda_\ell} \left[1 - \mu_\ell \cos^2(\alpha - \beta_\ell) \right]. \quad (\text{C-10})$$

Since equations (C-8) and (C-10) are identical, the rms-averaged velocity \tilde{V}_{nmo} is indeed equal to the exact NMO velocity in the linear approximation with respect to μ_ℓ [equation (C-6)].

APPENDIX D: THE DERIVATIVES OF GROUP VELOCITY WITH RESPECT TO THE RAY PARAMETERS γ_1 AND γ_2

Equation (59) contains the derivative of the group-velocity vector for the r -th mode ($r = 1, 2, 3$) in the ℓ -th layer [$\partial \mathbf{g}^{(\ell)} / \partial \gamma_n \equiv \partial \mathbf{g}^{(\ell, r)} / \partial \gamma_n$] with respect to the polar and azimuthal angles γ_1 and γ_2 of the unit wave-normal vector $\mathbf{n} = [\sin \gamma_1 \cos \gamma_2, \sin \gamma_1 \sin \gamma_2, \cos \gamma_1]$. Using equations (44) and (42), we find the following explicit representation:

$$\frac{\partial g_m^{(\ell, r)}}{\partial \gamma_n} = (a_{imkj} + a_{jmki}) \frac{\partial A_i^{(\ell, r)}}{\partial \gamma_n} p_k^{(\ell, r)} A_j^{(\ell, r)} + a_{imkj} A_i^{(\ell, r)} \frac{\partial p_k^{(\ell, r)}}{\partial \gamma_n} A_j^{(\ell, r)}, \quad (\text{D-1})$$

where the derivative $\partial p_k^{(\ell, r)} / \partial \gamma_n$ is defined by equation (60). The derivative of the polarization vector $\partial A_i^{(\ell, r)} / \partial \gamma_n$ can be found from equations (39) and (41) as

$$\frac{\partial A_i^{(\ell, r)}}{\partial \gamma_n} = \sum_{\substack{s=1 \\ s \neq r}}^3 d_{rs} A_i^{(\ell, s)}, \quad (n = 1, 2; i = 1, 2, 3), \quad (\text{D-2})$$

where

$$d_{rs} = \frac{V_r^2}{V_r^2 - V_s^2} (a_{imkj} + a_{ikmj}) A_i^{(\ell, s)} \frac{\partial p_m^{(\ell, r)}}{\partial \gamma_n} p_k^{(\ell, r)} A_j^{(\ell, r)}, \quad (s, r = 1, 2, 3; s \neq r). \quad (\text{D-3})$$